



ULUSLARARASI 3B YAZICI TEKNOLOJİLERİ  
VE DİJİTAL ENDÜSTRİ DERGİSİ

INTERNATIONAL JOURNAL OF 3D PRINTING  
TECHNOLOGIES AND DIGITAL INDUSTRY

ISSN:2602-3350 (Online)

URL: <https://dergipark.org.tr/ij3dptdi>

# INVESTIGATION OF ENERGY GENERATION FROM INCREASED WIND VELOCITY WITH BUILDING GEOMETRIES USING COMPUTATIONAL FLUID DYNAMICS AND WEIBULL FUNCTION

**Yazarlar (Authors):** Mehmet Bakırcı<sup>id</sup>, Noor Adil Mohammed<sup>id</sup>\*



**Bu makaleye şu şekilde atıfta bulunabilirsiniz (To cite to this article):** Bakırcı M., Mohammed N. A., "Investigation of Energy Generation From Increased Wind Velocity With Building Geometries Using Computational Fluid Dynamics and Weibull Function" *Int. J. of 3D Printing Tech. Dig. Ind.*, 7(1): 129-141, (2023).

DOI: 10.46519/ij3dptdi.1171463

Araştırma Makale/ Research Article

Erişim Linki: (To link to this article): <https://dergipark.org.tr/en/pub/ij3dptdi/archive>

# INVESTIGATION OF ENERGY GENERATION FROM INCREASED WIND VELOCITY WITH BUILDING GEOMETRIES USING COMPUTATIONAL FLUID DYNAMICS AND WEIBULL FUNCTION

Mehmet Bakırcı<sup>a</sup>, Noor Adil Mohammed<sup>a</sup>

<sup>a</sup>Karabük University, Faculty of Engineering, Mechanical Engineering Department, TURKEY

\* Corresponding Author: [nuram9559@gmail.com](mailto:nuram9559@gmail.com)

(Received: 06.09.2022; Revised: 05.12.2022; Accepted: 26.04.2023)

---

## ABSTRACT

Recently, humans have resorted to the use of renewable energies for the purpose of reducing global warming problems that affect the safety of the environment. Wind energy has started to occur in the first place among renewable energy types. However, it is difficult to obtain wind energy in areas where the wind speed is relatively low, so this study dealt with how to increase the production of wind energy in areas where the wind speed is relatively low by designing buildings that increase the wind speed by using of the phenomenon of venturi. How wide the high velocity values take place, how homogenous the distribution of the velocity is, and the turbulence values were calculated by CFD for four cases. It has been determined which of the four cases in which the wind turbine selected can operate most efficiently. One-year wind speed data measured at 10 m above the ground were taken from the Karabük Ovacık meteorological station. Annual energy calculations were made using the power characteristics of the selected wind turbine and Weibull graphs. It has been concluded that the amount of energy that can be obtained with the proposed building geometry layout in the mentioned region can be increased by 4 times.

**Keywords:** Wind Turbine, Buildings, Windspeed, Venturi Effect, Weibull, CFD.

---

## 1. INTRODUCTION

The rapid development of technology, science, and industries, as well as the occurrence of significant improvements in the standard of living, have greatly increased human needs in the areas of planning and living[1]. The need for energy has also increased to keep pace with the developments that have occurred recently, leading people to consume fossil energy greatly, but there are significant negatives such as environmental pollution caused by carbon dioxide released into the atmosphere, and high costs. After the occurrence of oil crisis in 1973, oil costs also increased. Therefore, people were forced to find inexpensive and environmentally friendly energy, so they started relying on a new energy source, which has been called renewable energy [2]. The use of renewable energy has spread widely in the world, as special complexes have been established to invest this energy[3]. This energy come from the sun, wind, and soil. Wind energy is one of the types of renewable energy that does not emit gases

that cause global warming[4]. It is extracted from the kinetic energy of the wind by means of wind turbines to produce electrical energy, as it is considered abundant and renewable energy [5]. The wind turbines are installed especially in regions where annual wind power distribution is sufficient. It is important to choose turbines compatible with annual statistical data of wind speed[6]. While vertical axis wind turbines are selected in regions where the wind speed changes frequently, horizontal axis wind turbines are selected to take advantage of the increasing wind speed as it rises from the ground [7]. For local electricity needs, turbines that are small and have a battery system for energy storage can be used. However, in areas with high wind speed throughout the year, commercial large wind turbines connected to the grid are used [8]. Wind turbines cannot be used in residential areas due to buildings and other obstacles that negatively affect wind speed. In addition, there are negative effects such as noise [9]. However, due to the increase

in wind speed with height, special designs have been applied in very high buildings, and applications have been made by placing turbines in the buildings and meeting some of the building's electricity needs [10]. In addition, successful results have been achieved in obtaining energy from the wind placing turbines while adding special designs to the roofs of buildings that are not very high [11]. There are also studies to obtain energy from vertical air movement on building facades by placing specially designed wind turbines on the side surfaces of the buildings [12]. There are experimental and CFD studies in the literature investigating and analysing how the wind moves around buildings [13]. In some of these studies, how the comfort of life inside the building is affected by the air movement outside the building was examined, while in another part, how the wind affects the building statics, especially in high-rise buildings was investigated [14–16].

Many studies examining the increase in velocity of the air by narrowing the distance between buildings with Computational Fluid Dynamics (CFD) are encountered in the literature. This is also called the venturi effect [15–18].

The focus of this study has been on benefiting from the wind energy in areas where the wind velocity is relatively low, not enough to operate wind turbines. It can be done by suitable placement of buildings in order to get the venturi effect. The buildings have been placed in a semi-parallel manner, and an attempt was made to narrow some areas of the buildings in order to increase the velocity of the wind flow. Four different cases were obtained by symmetrical placement of four different placement of building geometries in this study. They were analysed by CFD. After comparing the results of CFD study for the four cases of the buildings, the most suitable case has been chosen, and the power at which the wind turbines start to operate was checked. Finally, graphs were presented about Weibull distribution and the annual energy production. The main objective of this study is to fill in the existing literature gap on how to benefit from wind energy even in areas where the wind speed is low.

## 1.1. Theoretical Background

### 1.1.1 Mass Conservation

The conservation of fluid mass principle states that the product of density, velocity and cross-sectional area of the fluid passing through a certain cross-section will remain constant. This creates the possibility of increasing the low wind speed by placing the two building geometries in a way that narrows the cross-sectional area [19].

According to the law of conservation of mass, the mass flow of a fluid (air) for steady flow is

$$\sum_{in} m = \sum_{out} m \quad (1)$$

Where  $m_1 = m_2$  When  $m_2$  Indicates mass flow rate of fluid (air) (kg/sec).

$$m_1 = Q_1 \rho_1 \quad (2)$$

$Q_1$  Is the volume flow rate ( $m^3/sec$ )

Whereas  $Q_1 = V_1 A_1$ ,  $V$  is the velocity of air (m/sec).  $A$  is the cross-section area ( $m^2$ )

So  $m_1 = \rho_1 V_1 A_1$ .

$$\rho_1 V_1 A_1 = \rho_2 V_2 A_2 \quad (3)$$

So  $V_1 A_1 = V_2 A_2$  because the fluid (air) is incompressible in this case.

From here, it was reached that the smaller the area, the velocity increases, that is, the proportionality between the fluid velocity and the cross-sectional area is reversed. Accordingly, the design of the buildings has been chosen and the area where the air velocity reaches the highest possible was determined for the purpose of operating the wind turbines.

### 1.1.2. Weibull Distribution

In a given location, the wind speed does not remain constant throughout the year. So how much energy is obtained from the wind blowing in this place during a year is related to how the wind speed changes throughout the year. This evaluation is mostly done with the Weibull distribution [20].

The Weibull probability graph is obtained through the use of Equation (4) by taking the hourly average speed values in the measurements made during the year (in order to

obtain more reliable results, or a few years) in the region where the turbine will be installed[21].

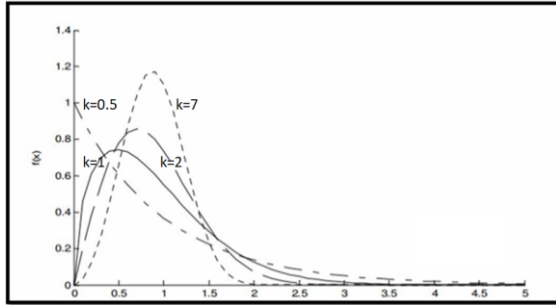


**Figure 1.** Graphs by parameters of the Weibull distribution[22].

For  $v_i < v < v_{i+1}$

$$p(v_i < v < v_{i+1}) = \exp\left(-\left[\left(\frac{v_i}{A}\right)^k\right]\right) - \exp\left(-\left[\left(\frac{v_{i+1}}{A}\right)^k\right]\right) \quad (4)$$

Where A and k are found for a given site on the Equation(4) [23].

In this function k and A values are measurements of how wind velocity is distributed in a year. Every placement has its own k and A values. Weibull graphs shows the relation between probability and velocity values, for different k values, shown in the figure 1 [22]. A wind turbine should be chosen according to the Weibull distribution.

In this study, k and A values were calculated as 1.2 and 7 respectively by using the wind data values at the meteorology station for Karabük-Ovacık in 2021.

**1.1.3. Efficiency of wind turbine**

The amount of energy to be obtained in a year from a wind turbine installed in a certain location depends on the Weibull values at that location, and also on the efficiency and power curve of the wind turbine. The overall efficiency of the turbine depends on rotor aerodynamic efficiency, mechanical efficiency and electrical efficiency. These efficiencies are shown mathematically in the equations[23].

From Betz’s equations about the maximum power available in the wind [24]. Power is defined as Equation. (5).

$$P_{max} = \frac{16}{27} \frac{1}{2} \rho \cdot v_1^3 \cdot A \quad (5)$$

Where  $C_p = C_{p,Betz} = 16/27$  was used .

In Equation (5) A is the swept area of the rotor, and in the following we define this area as

$A = (\pi/4) \cdot D^2$  (It has been neglected that some part of the hub area is not producing any power).

The rotor efficiency is defined as.

$$\eta_{max} = \frac{P_{rotor}}{P_{max}} \quad (6)$$

Where  $P_{rotor}$  is the power in the rotor shaft.

The rotor efficiency can be calculated on the basis of a Blade Element Momentum (BEM) Theory. The efficiency of the rotor is derived from the product of three efficiencies. As shown in Equation (7).

$$\eta_{rotor} = \eta_{wake} \cdot \eta_{tip} \cdot \eta_{profile} \quad (7)$$

Where “wake” indicates the loss because of rotation of the wake, “tip” represents the tip loss and “profile” represents the profile losses. The wake loss can be calculated on the basis of Schmitz’ theory [23].

Figure 2. indicates the components of a wind turbine.

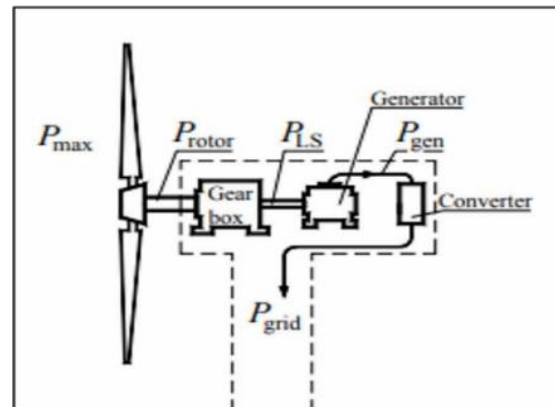


**Figure 2.** Main components in wind turbine[22].

The total efficiency of such a turbine can be defined as Equation (8).

$$\eta_{total} = \frac{P_{grid}}{P_{max}} = \eta_{rotor} \cdot \eta_{gearbox} \cdot \eta_{gen} \cdot \eta_{conv} \quad (8)$$

Where

$$\eta_{rotor} = \frac{P_{rotor}}{P_{max}}$$

$$\eta_{gearbox} = \frac{P_{HS}}{P_{rotor}}$$

$$\eta_{gen} = \frac{P_{gen}}{P_{HS}}$$

$$\eta_{conv} = \frac{P_{grid}}{P_{gen}}$$

Where the indices stand for “LS” = low speed (shaft); “gen” = generator; “conv” = frequency converter and “grid” = grid net. So typical values for the efficiencies are – at nominal power Gearbox:0.95-0.98, Generator: 0.95-0.97, Converter: 0,96-0,98 at part load, the lower values can be expected[22].

In this study, maximum efficiency ( $\eta_{max}$ ) of the wind turbine chosen is 0.4.

The turbine power curve shows at which wind speed the turbine starts to operate (cut in), after which wind speed it is stopped (cut out), and in which wind speed range it produces maximum (nominal) power. This characteristic is a result of turbine efficiency values and design parameters [23].

In this study, cut in velocity, cut out velocity, nominal velocity of the selected wind turbine are 3 m/s, 26 m/s, 11 m/s respectively.

#### 1.1.4. Annual Energy Calculation

The energy that the turbine can produce in a year depends on the wind speed statistics of the region where the turbine is located and the power graph of the turbine. The total amount of energy that can be obtained annually is calculated by the Equation (9)[23].

If the power for the turbine at a given wind speed is  $P(v_m)$ , the annual production can be calculated as:

$$E_{ann} = \sum\{8766h. p(v_i < v < v_{i+1}). P(v_m)\} \quad (9)$$

Where  $v_m$  is the mean value of  $v_i$  and  $v_{i+1}$  i.e.

$$v_m = (v_i + v_{i+1})/2$$

#### 1.1.5. Wind homogeneity and turbine efficiency

Frequent changes in the magnitude and/or direction of the wind speed over time cause the turbine rotor to be under the influence of inhomogeneous wind. This situation negatively affects the energy to be obtained from the turbine. Therefore, the homogeneity of the wind should be taken into account in the place where the turbine will be installed[25].

#### 1.2. Computational Fluid Dynamics (CFD)

Computational Fluid Dynamics is based on the numerical solution of partial differential equations expressing the conservation of mass, momentum and energy of fluids in a large number of cells created in the defined flow area. Boundary conditions of the defined flow area are defined[26].

In this study, inlet boundary velocity, output boundary pressure, solid surfaces ‘wall’, and flow field boundaries ‘symmetry’ are defined, and conservation equations are solved in the cells (mesh) created, and velocity in each cell, static pressure values as well as turbulence kinetics are determined. Energy equations are not solved in this study. Because energy equations are solved in analyses involving heat and temperature and/or compressible fluid analysis.

In CFD calculations, there are three basic calculation methods: Reynolds-Averaged Navier-Stokes (RANS), Large Eddy Simulation (LES) and Detached Eddy Simulation (DES). RANS equations are the most widely used CFD approach for practical engineering applications. They solve for time-averaged flow properties and are typically used for steady-state simulations. However, this approach is not suitable for predicting unsteady or transient flow phenomena, where large fluctuations in the turbulent flow field can have a significant impact on the results. The choice of CFD approach depends on the specific application and the level of accuracy required. RANS is the most widely used and computationally efficient CFD approach for practical engineering applications, while LES and DES are more suitable for predicting unsteady or transient flow phenomena and complex flow regions [27]. The easiest and most widely used RANS was used in this study.

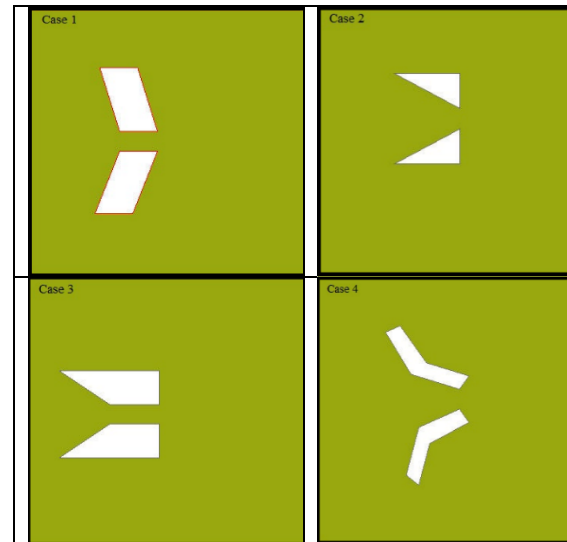
The most common turbulence models used in RANS simulations are the Spalart-Allmaras, k-omega, and k-epsilon models. The Spalart-Allmaras model is a one-equation model that solves for a single variable to represent the turbulent viscosity, and it is particularly useful for attached boundary layers and external flows. The k-omega model is a two-equation model that solves for both the turbulent kinetic energy (k) and the specific dissipation rate (omega), and it is particularly useful for flows with strong vortices and shear layers. The k-epsilon model is also a two-equation model that solves for the turbulent kinetic energy (k) and the rate of dissipation of turbulence kinetic energy (epsilon), and it is particularly useful for flows with complex turbulence structures.

There are also many sub-varieties of these models, which include modifications and enhancements to improve their accuracy or to account for specific flow characteristics. For example, the RNG k-epsilon model is a modification of the standard k-epsilon model that includes additional terms to improve its performance in swirling flows. The SST k-omega model is a hybrid model that combines aspects of both the k-epsilon and k-omega models to improve its accuracy in a wide range of flow regimes [28]. In present CFD simulations, the SST k-omega model was used.

## 2. METHOD

### 2.1. Numerical Calculations

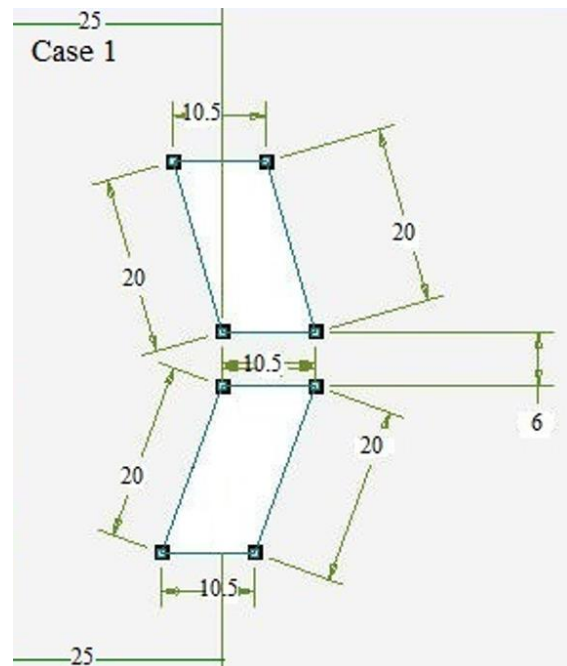
From the literature[29], four different two-dimensional (top view) building geometries were taken, and four different cases were obtained by bringing together two symmetrical buildings as shown in the figure 3.



**Figure 3.** The geometry of the four cases of the buildings [25].

For these four cases, flow fields were created as shown in the figure. On the left edges of these flow areas, the wind entering edge, the wind entry velocity is defined. Since this study is for regions with low wind speed, the velocity values taken are 2, 4, 6 m/s.

The dimensions of four different cases are shown in the figure 4.



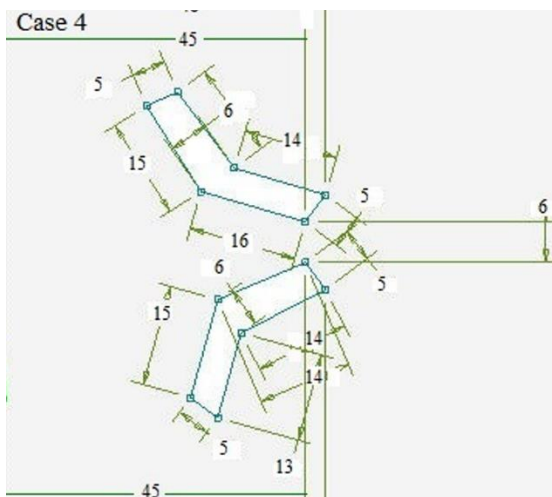
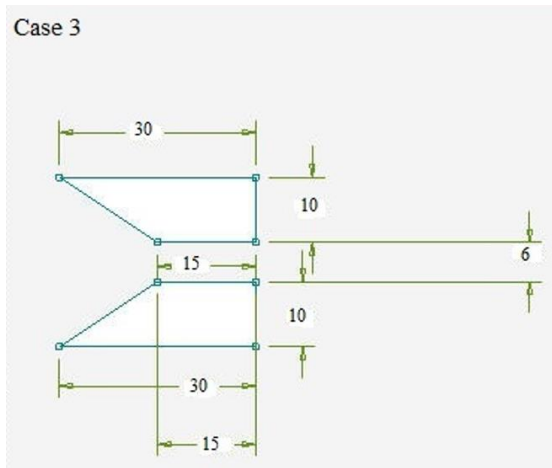
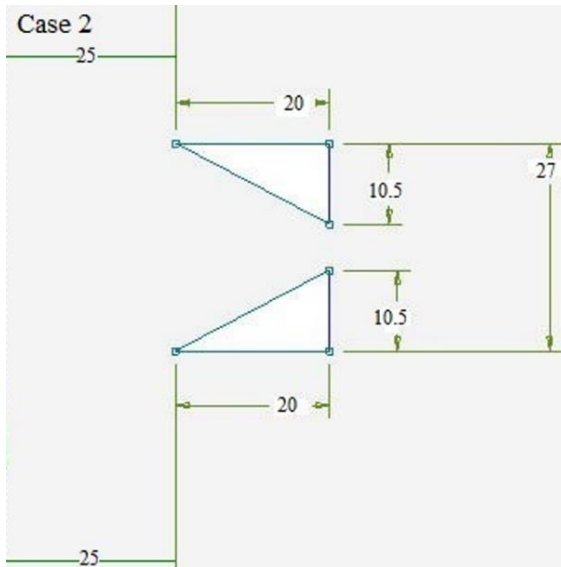


**Figure 4.** The geometry of the four cases of the buildings that were studied with their parameters.

The fluid domain used in this CFD simulation is shown in Figure 5. The left edges of the flow field are named as ‘inlets’. For ‘inlet’, the wind is defined as perpendicular to the left edge with the speed value. The building geometries are

defined as ‘wall’, the upper and lower edges of the flow area are defined as ‘symmetry’ and the right edges are defined as ‘outlets’. Zero effective pressure value is taken for the outlet.

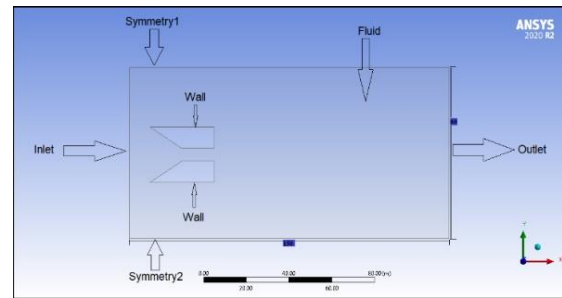


**Figure 5.** Named sections of the geometry.

## 2.2. Mesh quality and independence

There are different methods to see the accuracy of the results obtained from the computational fluid dynamics analysis. The most important of these are validation, comparison of calculation results with theoretical formulas, comparison with test results for the same geometries and under the same conditions. However, verification, on the other hand, is one of the most important ones to show whether the computational fluid dynamics results are consistent within themselves or not, to show that the quality of the cells created in the flow field is good enough and to show that the results obtained do not change when the number of cells is increased[31]. Figure 6 indicates the mesh structure in Case3.

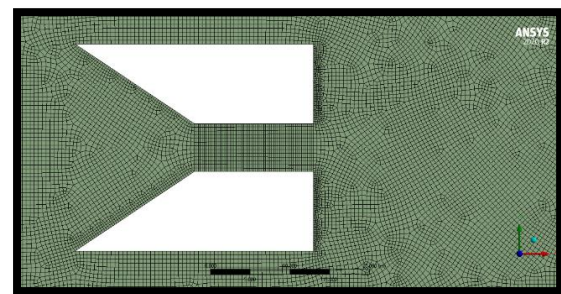


**Figure 6.** Mesh structure.

When the mesh number was increased from 2000 to 7000, it was seen that the results (output velocity values) changed very little and after 7000 cells the results did not change at all (Figure 7). Apart from this, in order to have high mesh quality in CFD simulations, it is recommended to have skewness values below 0.5 and orthogonality values above 0.7 [31]. In the CFD study conducted here, it was ensured that the mesh quality was high enough.

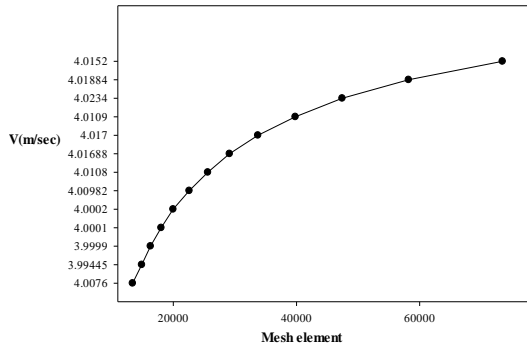


Figure 7. Mesh independence test.

**2.3. Setup**

The following physical conditions and numerical solution criteria are taken into account in the computational fluid dynamics solution:

- 1.The solution was taken as steady.
- 2.Energy was turned off.
3. Viscous Model is k- $\omega$  (SST). It was chosen because it achieves better and more accurate results when the mesh is very fine near the wall [32].
- 4.Boundary conditions:
  - At inlet velocity is (2,4,6 m/sec)
  - In this study, walls are designed as no-slip
  - Neglected direction of velocity
- 5.Solution method is coupled
- 6.Number of iterations is 500.

**3. RESULTS AND DISCUSSIONS**

The maximum wind speed values that can be obtained between and around the building geometries were calculated using the same inlet speeds in four different situations (Table 1).

**Table 1.** Maximum velocity flow for four cases to the buildings.

Inlet Velocity (m/sec)	Case1	Case2	Case3	Case4
2	6.64	4.04	5.18	5.91
4	13.3	8.07	9.77	12.2
6	20	12.7	15.3	18.3

While the largest maximum speed values for all input speeds were obtained in Case1, the smallest maximum speed values were obtained in Case2. But this does not necessarily mean that Case1 is the best one.

The case of wind turbine placement cannot be evaluated based on this result alone. Because the general distribution and homogeneity of the wind speed to which the turbine rotor is exposed, as well as the turbulence situation should also be taken into account.

For the Case1, we can see how the velocity value changes around the building geometry from the contour graph given in figure 8.

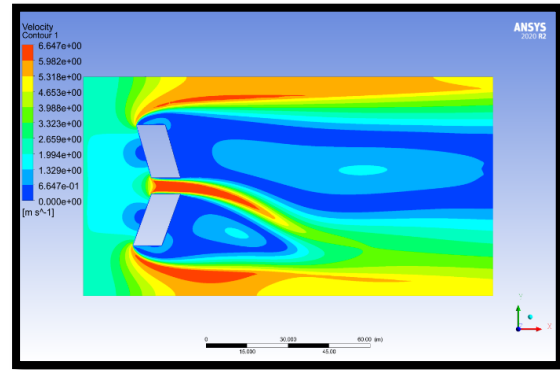


Figure 8. Velocity contour in Case1.

In Case1, when looking at the streamlines, vortices formed around the building geometries can be noticed. As shown in Figure 9.

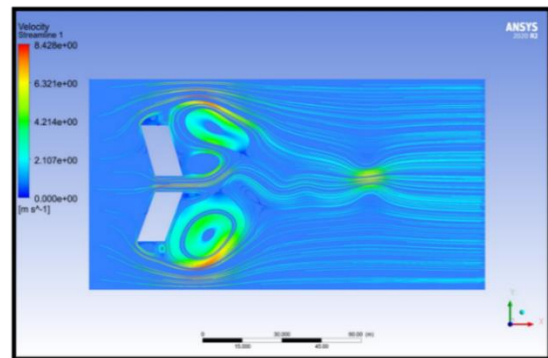


Figure 9. Streamline contour for velocity Case1.

It can be concluded that, in Case1, the velocity distribution does not have enough homogeneity and stable velocity although it has the largest maximum velocity value.

Therefore, how wide the highest speed values are spread, how the distribution of high-speed values is in the section where the turbine can be placed between two buildings, what the turbulence values are will affect the efficiency of the turbine to be used. All these properties of the flow around the building geometries were investigated in CFD study. When all of this



criterion was analysed for four different cases, Case 3 was found to be the best.

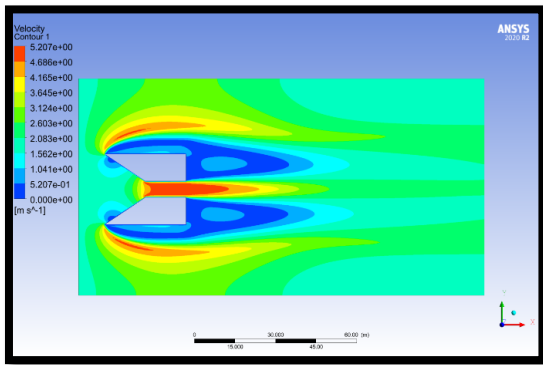


Figure 10. Velocity contour in Case3.

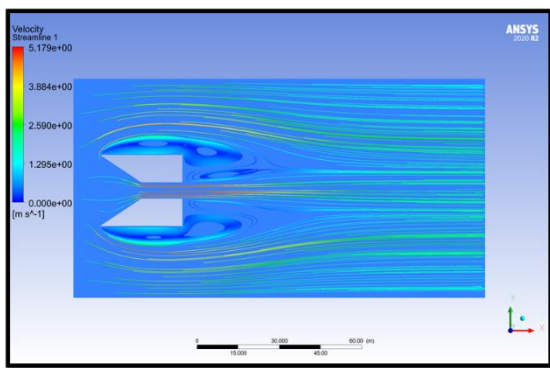


Figure 11. Streamline of Velocity contour for Case3.

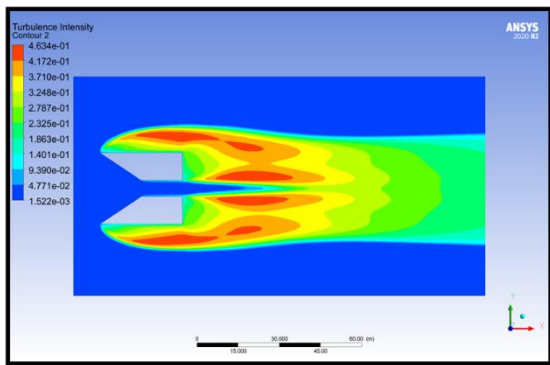


Figure 12. Turbulence intensity contour for Case3.

How the velocity values for the Case3 change around the two buildings can be seen from the velocity contour shown in figure 10 and the velocity streamlines shown in figure 11. Also, considering the turbulent kinetic energy distribution contour shown in Figure 12, the low values between the two buildings and the homogeneous velocity distribution give a clue that the Case3 may be suitable for turbine installation. Therefore, Case3 should be examined more closely.

The velocity distributions and turbulent kinetic energy changes between and around the buildings for four different cases were examined and it was concluded that the most favourable situation would be obtained in the Case3 with homogeneous velocity distribution of high velocity values.

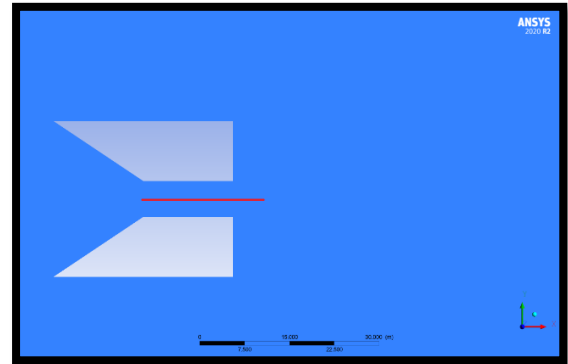


Figure 13. Pressure line.

The static pressure change on this line is shown in figure 13. It is seen that the pressure first decreases rapidly along the line and then does not change much. As shown in figure 14.

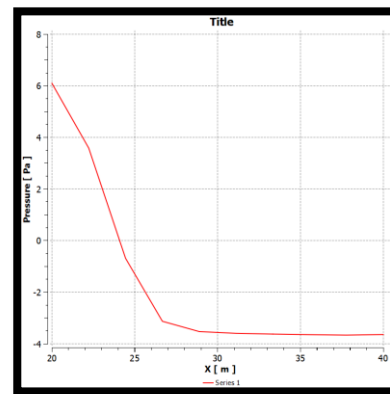
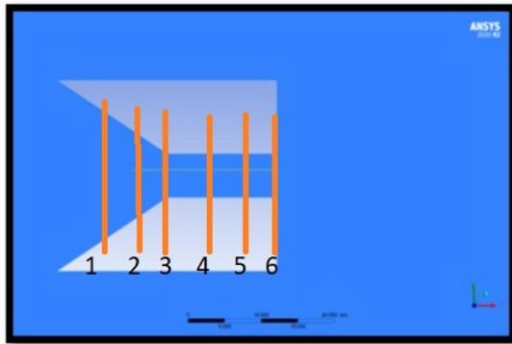


Figure 14. Pressure graphic between two buildings on the pressure line.

In order to specify the placement of the wind turbine in between the two buildings in Case3, pressure, velocity and turbulence conditions were examined in 6 different positions taken on the line drawn in the middle between the two buildings and the best position where the turbine could be placed was determined. Those positions are shown in the figure 15.



**Figure 15.** Lines for the possible positions of the wind turbine.

Figure 16 refers to the wind speed graphic at the six positions identified in Figure 15.

It was found that the wind speed increases gradually at the 4<sup>th</sup>, 5<sup>th</sup> and 6<sup>th</sup> position, especially in the side that is in the middle of the two buildings and achieves the highest value at the line 6. As shown in the graphics, the wind speed starts to increase at one of the buildings until it reaches an area in the middle of the two buildings, where it will see a state of stability in the wind speed, but then it gradually decreases when it reaches the edge of another building. The wind speed has been studied in the six sites in order to discover that the high wind speed is maintained for long distances between the two buildings for the purpose of selecting the appropriate wind turbines.

Figure 17 shows the graphic of wind turbulence between the two buildings at position 6 that were previously divided. Whereas it is necessary to study wind turbulence and its amount, because wind turbulence has a great impact on the work of wind turbines, as wind turbulence causes vibrations and fatigue in the turbine blades, which leads to reducing efficiency and increasing wear in the turbines. It was noticed that the wind turbulence graphic is opposite to the wind speed graphic. The turbulence begins with its highest value at the edge of the one of building. It gradually decreases in the central region between the two buildings, and then gradually increases until it reaches the edge of another building. The two graphics have been studied in detail for the purpose of determining the appropriate area for placing the wind turbine, as well as determining the type of turbine suitable for this study and its dimensions. Table 2 indicates the value of velocity and turbulence at position 6 that were previously divided.

**Table 2.** Velocity value and Turbulence intensity in each line.

Line	Velocity (m/sec)	Turbulence intensity
1	1.80641	0.006
2	4.02142	0.016
3	4.2449	0.028
4	4.25129	0.027
5	4.25726	0.028
6	4.43688	0.109

The distribution of velocity values and turbulence intensity values obtained as a result of computational fluid dynamics analysis at these 6 different locations are compared with graphs (Figures 16 and 17). It can be said that the position where the highest velocity is obtained, the velocity distribution is most homogeneous, and the lowest turbulent intensity value is obtained is line 2.

Since the distance at the selected location between the two buildings where the turbine can be placed is slightly more than 6 m, the turbine rotor diameter can be chosen as 5 m. The selected horizontal axis wind turbine has a start speed (cut in) of 3 m/s, stop speed (cut out) of 26 m/s, nominal speed of 11 m/s. Its rated power is 1.22 kWatt. The power curve of this turbine is shown in figure 18.

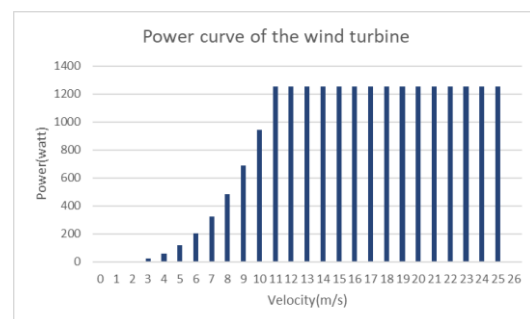


**Figure 18.** Annual power of wind turbine.

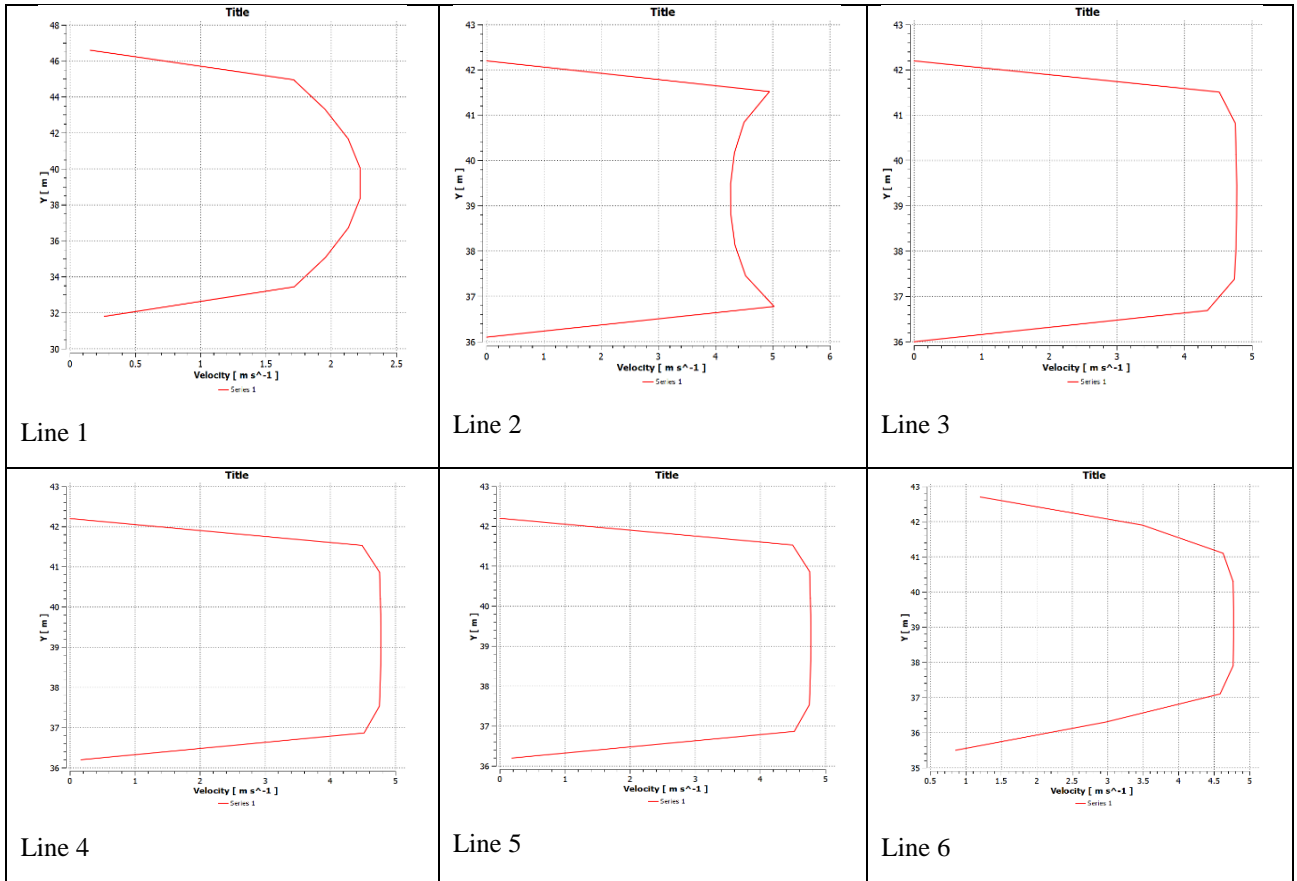


Figure 16. Diagrams of the velocity flow between two buildings in each of the lines (1,2,3,4,5,6) respectively.

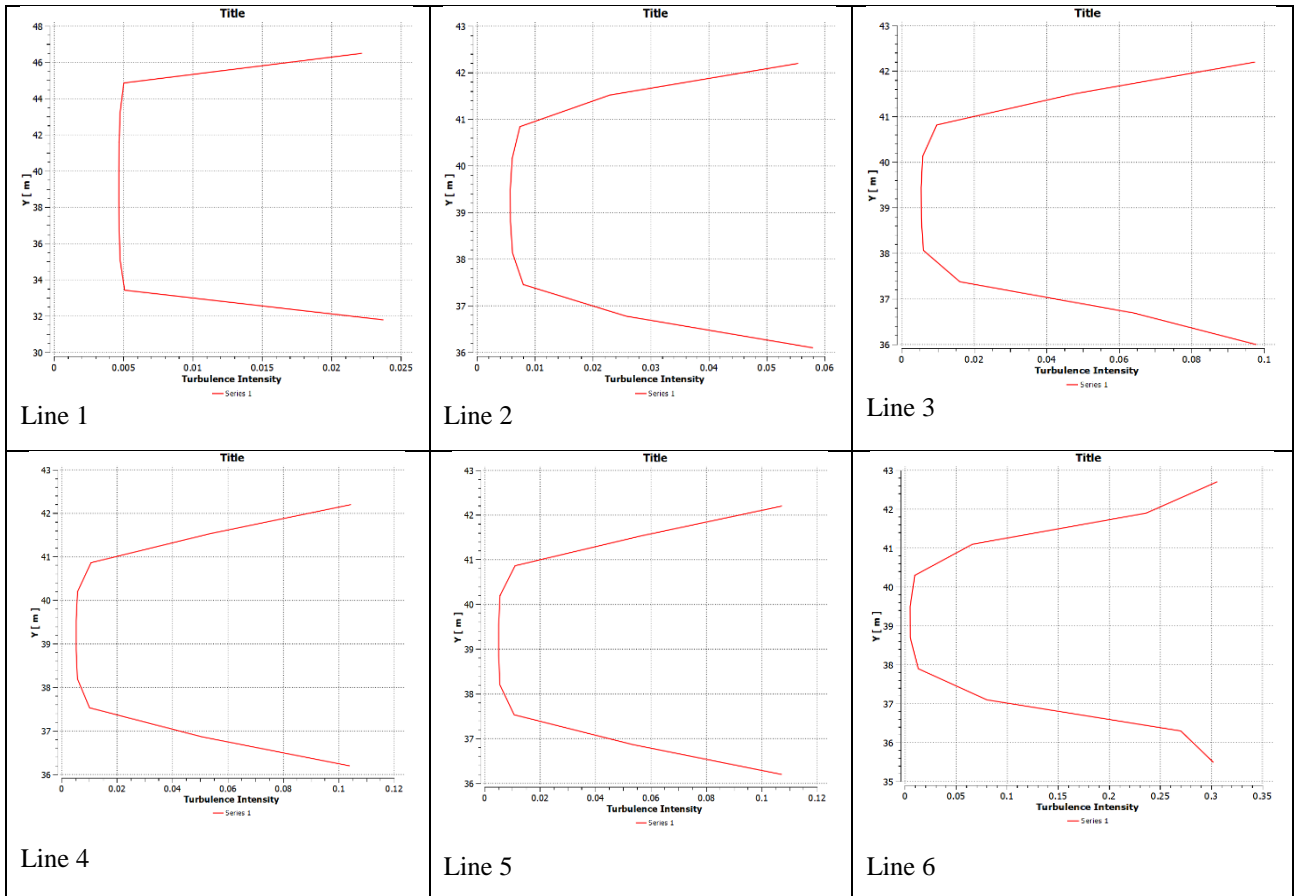
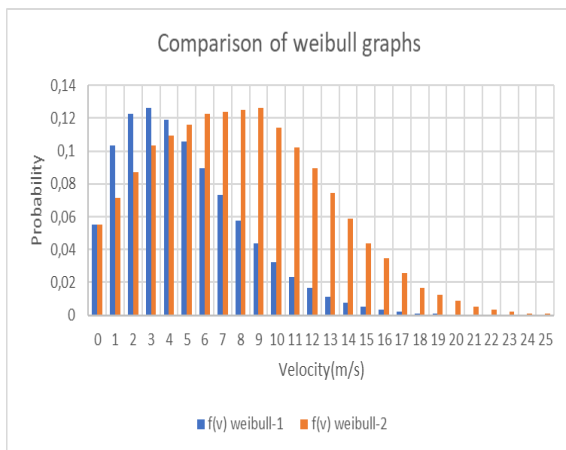


Figure 17. Diagrams of the turbulence intensity between two buildings in each of the lines ((1,2,3,4,5,6) respectively.

As a suitable example for the low wind speeds mentioned in this study, energy calculations were made using one-year wind speed data obtained from the meteorology station located in the Ovacık region of Karabük province. New speed values were obtained by interpolation, considering the wind speeds of this region and the results of the Case2 analysed with computational fluid dynamics. The Weibull distributions of the velocity values of the region at a height of 10 m and the two building placements in Case3 were obtained and compared as shown in Figure 19.



**Figure 19.** A windspeed probability density function.

It is seen that the velocity values between 1 m/s and 19 m/s in the region reached values between 1 m/s and 29 m/s with the placement of the two buildings as in Case3 (Figure 19). More importantly, it can be seen from the graphs given in Figure 19 that the Weibull probability values increase for the turbine's operating range of 3 m/s and 24 m/s speed values (especially for the speed range between 3 m/s and 19 m/s).

When the annual energy calculation is made for Case2, the amount of energy (energy-1) obtained by the wind turbine (shown in blue) at different wind speeds in the region without the venturi effect and the amount of energy (energy-2) obtained by the same wind turbine (shown in green) according to the new speed values obtained by placing two buildings are compared. Graphics are given in Figure 20.

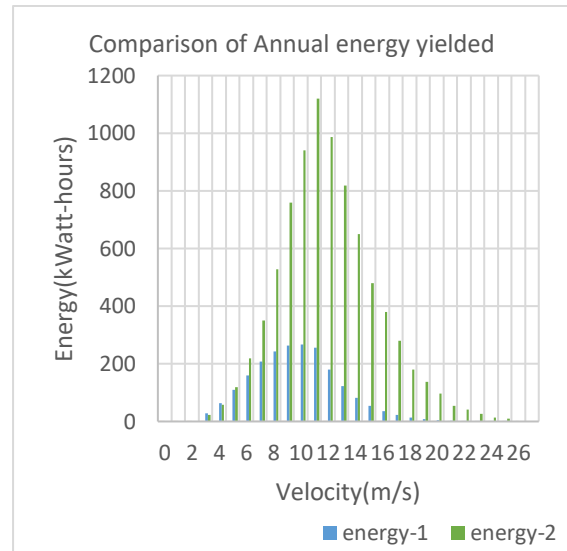


**Figure 20.** Annual power production.

#### 4. CONCLUSION

In this study, a solution has been proposed to meet some of the electricity needs of the buildings in regions where the wind speed is not sufficient to operate the wind turbine efficiently and where a new settlement can be established. The creation of a venturi effect by placing two symmetrical buildings in the direction of the wind was analysed by computational fluid dynamics. Four different situations were created with four different building geometries, and the wind speeds of 2, 4, 6 m/s in each of them were calculated by CFD, up to which speeds could be increased by the venturi effect. The homogeneity of the wind and the turbulence situation were also analysed to determine the state where the turbine can operate most efficiently. Since there is a 6 m gap between the two buildings, a 5 m diameter horizontal axis wind turbine installed on a 10 m high tower was chosen.

One-year wind speed data measured in the meteorological station area in the Ovacık region of Karabük province and Weibull statistical graphics for the new speed values obtained as a result of CFD analyses were used to calculate the amount of energy that can be obtained in this region for a year, and the results were compared.

While the amount of energy that can be obtained in a year with a wind turbine with a diameter of 5 m and used in this chosen location is 2126.58 kWh, this amount increases to 8272.58 kWh with the effect of venturi resulting from the proper placement of the buildings. It

has been observed that the amount of energy that can be obtained with the proposed building layout in the mentioned region can be increased by approximately 4 times.

In this study, the change of wind direction was not taken into account. The heights of the buildings were not taken into account in the CFD study. However, the speed of the wind increases as it rises from the ground.

If the wind direction values are taken into account in the data taken from the meteorology in a region taken as an example, more accurate results will be achieved. Taking into account the roughness coefficient values of the region will cause the study results to be more reliable.

Considering the heights of the buildings, more accurate results will be achieved if both the variation of wind speed with height and how the vertical surfaces of the buildings affect the air flows are taken into account.

## REFERENCES

1. IEA, "Key World Energy Statistics 2021 Statistics Report" IEA Publ., Pages 1–82, 2021.
2. Euclid A. Rose "OPEC's Dominance of the Global Oil Market: The Rise of the World's Dependency on Oil", *The Middle East Journal*, Vol. 58, Issue 3, Pages 424-443, 2004.
3. B. Bulut, "Remaining Useful Life Prediction in Wind Farms", *International Journal of 3D Printing, Technology and Digital Industry* Vol. 5, Issue 2, Pages 145–154, Aug. 2021.
4. S. Gorjian, "An Introduction to the Renewable Energy Resources", *Renewable Energy Technologies* Vol. 4, Pages 41-42, June. 2017.
5. IRENA, International Renewable Energy Agency, "Global renewable outlook - energy transformation 2050", 2020.
6. Department of Energy, "Wind Market Reports: 2021 Edition", <https://www.energy.gov/eere/wind/wind-market-reports-2021-edition>, 2021.
7. A. Iqbal, V. Chitturi, and K. V. L. Narayana, "A Novel Vertical Axis Wind Turbine for Energy Harvesting on the Highways", 2019 *Innov. Power Adv. Comput. Technol. i-PACT* 2019.
8. G. Boroumandjazi, R. Saidur, B. Rismanchi, and S. Mekhilef, "A review on the relation between the energy and exergy efficiency analysis and the technical characteristic of the renewable energy systems", *Renewable and Sustainable Energy Reviews*, Vol. 16, Issue 5, Pages 3131–3135, Jun. 2012.
9. C. M. Hsieh and C. K. Fu, "Evaluation of Locations for Small Wind Turbines in Coastal Urban Areas Based on a Wind Energy Potential Map", *Environmental Modeling and Assessment*, Vol. 18, Issue 5, Pages 593–604, 2013.
10. K. C. S. Kwok and G. Hu, "Wind energy system for buildings in an urban environment", *Journal of Wind Engineering and Industrial Aerodynamics*, Vol. 234, Issue(-), Pages 105349, Mar. 2023.
11. H. Zhu, B. Yang, Q. Zhang, L. Pan, and S. Sun, "Wind engineering for high-rise buildings: A review", *Wind and Structures. An International Journal*, Vol. 32, Issue 3, Pages 249–265, 2021.
12. T. Stathopoulos et al., "Urban wind energy: Some views on potential and challenges", *J. Wind Engineering Industrial Aerodynamics*, Vol. 179, Pages 146–157, Aug. 2018.
13. R. Djedjig, E. Bozonnet, and R. Belarbi, "Experimental study of the urban microclimate mitigation potential of green roofs and green walls in street Canyons", *International Journal of Low-Carbon Technologies*, Vol. 10, Issue 1, Pages. 34–44, 2015.
14. A. Aflaki, N. Mahyuddin, G. Manteghi, and M. Baharum, "Building Height Effects on Indoor Air Temperature and Velocity in High Rise Residential Buildings in Tropical Climate", *OIDA International Journal of Sustainable Development*, Vol. 07, Issue 07, Pages 39–48, 2014.
15. D. R. Bhola, "CFD analysis of flow through venturi of carburetor", *IJRMET* Vol. 4, Issue 2, Spl-2 May - October 2014.
16. B. Li, Z. Luo, M. Sandberg, and J. Liu, "Revisiting the 'Venturi effect' in passage ventilation between two non-parallel buildings", *Building and Environment*, Vol. 94, Issue November, Pages 714–722, 2015.
17. System Analysis Blog Cadence, "Explaining Venturi Effect Wind Flow Analysis in Structural Design", <https://resources.systemanalysis.cadence.com/blog/msa2022-explaining-the-venturi-effect-and-wind-flow-analysis-in-structural-design>, 2022.
18. A. Whiston "Urban Street Canyons", Harvard Graduate School of Design,

- [http://web.mit.edu/nature/archive/student\\_projects/2009/jcalamia/Frame/05\\_canyonwind.html](http://web.mit.edu/nature/archive/student_projects/2009/jcalamia/Frame/05_canyonwind.html) 1986.
19. R. S. Subramanian, "Engineering Bernoulli Equation", Department of Chemical and Biomolecular Engineering. Clarkson University., Pages. 1–19, 2014.  
<https://web2.clarkson.edu/projects/subramanian/ch330/notes/Engineering%20Bernoulli%20Equation.pdf>
  20. F. Oral, I. S. Ekmekçi, and N. Onat, "Weibull distribution for determination of wind analysis and energy production", *World Journal of Engineering*, Vol. 12, Issue 3, Pages 215–220, 2015.
  21. S. Heier "Wind Energy Conversion Systems", *Grid Integr. Wind Energy*, Pages 31–117, Apr. 2014.
  22. E. Dick, "Wind Turbines", *Fluid Mechanics and Its Applications*, Vol. 130, Issue June, Pages 371–396, 2022.
  23. N. Jenkins and A. Vaudin, "Wind Power Plants", *Wiley Encyclopedia of Electrical and Electronics Engineering*, Germany, 1999.
  24. E. Barlas, W. J. Zhu, W. Z. Shen, and S. J. Andersen, "Wind Turbine Noise Propagation Modelling: An Unsteady Approach", *Journal of Physics Conference Series*, Vol. 753, Issue 2, 2016.
  25. R. Gasch and J. Twele, "Wind power plants: Fundamentals, design, construction and operation, second edition", Pages 1–548, Springer Science and Business Media, Berlin, 2012.
  26. T. J. Chung, "Computational Fluid Dynamics", second edition, Vol. 9780521769., Cambridge University Press, Cambridge, 2010.
  27. M. Moshinsky, "Computational Methods for Fluid Dynamics", Vol. 13, Issue 1. 1959.
  28. F. R. Menter, "Two-equation eddy-viscosity turbulence models for engineering applications", *AIAA J.*, Vol. 32, Issue 8, Pages 1598–1605, 1994.
  29. Z. T. Ai, C. M. Mak, and J. L. Niu, "Numerical investigation of wind-induced airflow and interunit dispersion characteristics in multistory residential buildings", *Indoor Air*, Vol. 23, Issue 5, Pages 417–429, Oct. 2013.
  30. A. Chabas et al., "Long term exposure of self-cleaning and reference glass in an urban environment: A comparative assessment", *Build. Environ.*, Vol. 79, Pages 57–65, Sep. 2014.
  31. A. Samadi and H. Arvanaghi, "CFD simulation of flow over contracted compound arched rectangular sharp crested weirs", *Iran Univ. Sci. Technol.*, Vol. 4, Issue 4, Pages 549–560, 2014.
  32. H. Yu and J. The, "Validation and optimization of SST  $k-\omega$  turbulence model for pollutant dispersion within a building array", *Atmospheric Environment*, Vol. 145, Pages 225–238, Nov. 2016.